



CFD Modelling of Ionic Propulsion, the Electric Jet Engine

Jason Knight, Arundeeep Matharu, Nikesh Mehta, Ziaul Hoque,
Carlson Ddamba, David Bickersteth, James Buick, Ethan Krauss
and George Haritos

EasyChair preprints are intended for rapid dissemination of research results and are integrated with the rest of EasyChair.

May 23, 2023

CFD Modelling of Ionic Propulsion, The Electric Jet Engine

Jason Knight¹, Arundeeep Matharu¹, Nikesh Mehta¹, Ziaul Hoque¹, Carlson Ddamba¹,
David Bickersteth¹, James Buick¹, Ethan Krauss², George Haritos³

¹ University of Portsmouth, UK

² Electron Air LLC, USA

³ Kingston University, UK

Abstract. All aircraft engines work by pushing air backwards so that the aircraft moves forward. Ionic propulsion instead uses charged particles or ions that are generated using high voltages in between two electrodes. The ions interact with the surrounding air, creating an ionic wind that is sent backwards, propelling the aircraft forward. As with propeller-driven solar powered aircraft, ion drive craft are powered by electricity and do not need to carry fuel, other than batteries filled with charged particles. As well as being silent and carbon neutral, they are less likely to go wrong and cheaper to maintain than conventional engines because they have no propellers, turbines or fuel pumps to break down. The main challenge was that, in Earth's gravity, the thrust produced by ion drive wasn't enough to overcome the weight of the batteries needed to power it. However, with advances in battery setup and the way the electrical power is converted, it has been possible to reduce the battery weight enough to make this technology fly under its own power. The earlier VTOL version of the technology also required significant changes to its geometry, increasing thrust efficiency by about an order of magnitude, making onboard power possible. The use of Computational Fluid Dynamics to model the ionic wind can further improve efficiency. In this work we report the variation of lift to drag with change in vertical displacement of the emitter from the collector. Making further advances in aerodynamics, materials and power electronics could enable the aircraft to fly faster and for longer. It's likely the technology will find its first application in silent UAVs. Use in crewed flight will require significant further technological advances.

Keywords: Ionic Propulsion, Aerodynamics, Electrostatic.

1 Introduction

To date, ionic propulsion has been used primarily in space but it has also been used in Earth's atmosphere. There are generally 2 forms of ionic propulsion, which are Ion thrusters and Electro Aerodynamic Devices (EADs). Ion thrusters eject ions at very high velocities and are primarily used on satellites to change orbit. Further advances in the technology have been made and the latest development is the X3 prototype thruster which works by using multiple plasma rings [1]. EADs are used in the atmosphere and

use electricity to create an electrostatic field between an anode and a cathode [2]. In the electrostatic field, negatively charged ions are produced and repelled by the electrostatic force of the positively charged anode towards the negatively charged cathode. As they are repelled the ions collide with neutral particles in the fluid (air). The collisions induce a propulsive force, thus creating ionic wind [3]. EADs use this ionic wind to fly by either, directing it vertically downwards to generate lift and oppose its weight or by directing it horizontally to generate propulsion. In addition, if it is directed horizontally over a wing, additional lift is produced.

Ionic propulsion produces no pollution, provided the electricity it uses is generated by renewable energy. In addition, as there is no engine, noise pollution is minimal. Another benefit is that there are no moving parts meaning that less maintenance is required. The first aircraft with no moving parts was created in 1964 and was called the Ionocraft. The ionocraft produced an ionic wind that was propelled vertically downwards, generating lift and allowing it to fly. However, the power was supplied through a tethered cable, as no ion thruster produced a sufficient amount of power to lift off against Earth's gravity and sustain flight, carrying its power source. The first ionocraft with an onboard power supply was created by Ethan Krauss, Electron Air LLC in 2006 [4] as shown in Figure 1a, which was patented for lifting its power supply against Earth's gravity using ion propulsion [5]. The VTOL design requires an optimized efficiency geometry and a miniaturized electrical system [6].

In 2018, Massachusetts Institute of Technology (MIT) used the same technology in the horizontal plane to power a model of 5m wingspan, which is shown in Figure 1b. Their design converted the battery voltage of -225V to 40kV, which was output to the electrodes [7]. This provided up to 565W of power, with an efficiency of 85% and specific power of 1.15 kW/kg [8]. The design utilizes an array of cathodes (wires) in front of the anodes (airfoils). The MIT craft produced approximately 3.2N per 620 watts ($\frac{1}{2}$ gram of force per watt.) [9].

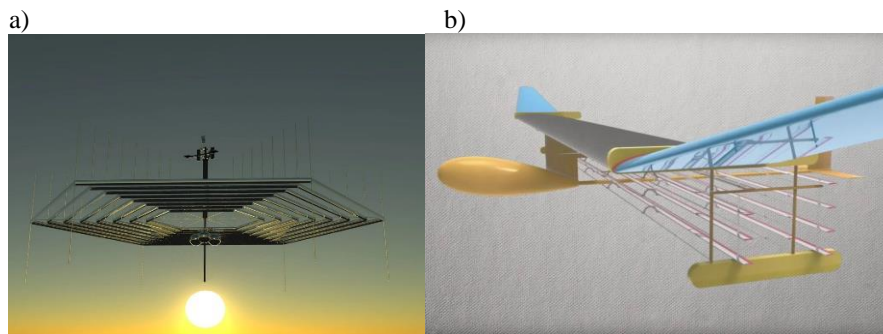


Fig. 1. Illustrations of EAD's by a) Electron Air LLC and b) MIT

2 Simulation Methodology

2.1 Model Setup and Geometry

We follow a similar approach to MIT and created geometry within Star CCM+ consisting of a wire and an airfoil. The wire was set as the emitter or anode and the airfoil as the collector or cathode, drawing the positively ionized particles towards the direction of the negatively charged airfoil. The airfoil selected for this simulation was the NACA 2412 with a chord length of 100mm.

A CFD model in two dimensions was created to simulate how the ionic wind created by the electro-aerodynamic thrust interacts with the airfoil to generate lift. Figure 2 shows the geometry and mesh that was created for the CFD simulation with the ionization region formed around the wire. The ionization region is the square root of the radius of the wire [10]. The wire radius used in the CFD model was 20 microns, which gave an ionization region thickness of 4.47 mm, which was located 12mm upstream of the airfoil. This is shown by the circle set upstream from the airfoil in the in Figure 2. The ionization region was set as an inlet with 1.04m/s, which was obtained by using equations derived from Wilson et al [10] with a supply voltage of 4kV. The inlet velocity was applied using cosine function so that maximum value was in the horizontal direction when the wire was at zero degrees or in the same horizontal plane as the airfoil. This was done in order to simulate the ionic flow being attracted to the collector in a similar fashion as the electro-magnetic field. The airfoil was set as a non-slip wall, allowing for the air from the inlet to pass around it. The upstream boundary was also set as an inlet with a velocity of 1m/s also applied in the horizontal direction. This helped with convergence of the CFD solution and it stopped the flow from creating vortices and circling back round on itself. An outlet was set downstream of the airfoil to allow the air to escape the region. Symmetry boundaries were applied at the ceiling and floor of the domain.

2.2 Mesh Convergence

The simulation was carried out using Star CCM+ to obtain lift and drag values. A mesh convergence study was made altering the base size and the number of prism layers on the surface of the airfoil. A base size of 0.005m was found to be sufficient with 5 prism layers, which resulted in y^+ values within the acceptable range of the law of wall constraints. Figure 2 shows the mesh used for the analysis with the emitter at zero degrees in front of the airfoil. The mesh is more refined in the space between the emitter and airfoil and also in the wake behind the airfoil, as these were the key areas where the airflow would be affected. The wake angle was set to 15° for a length of 0.5m behind the airfoil.

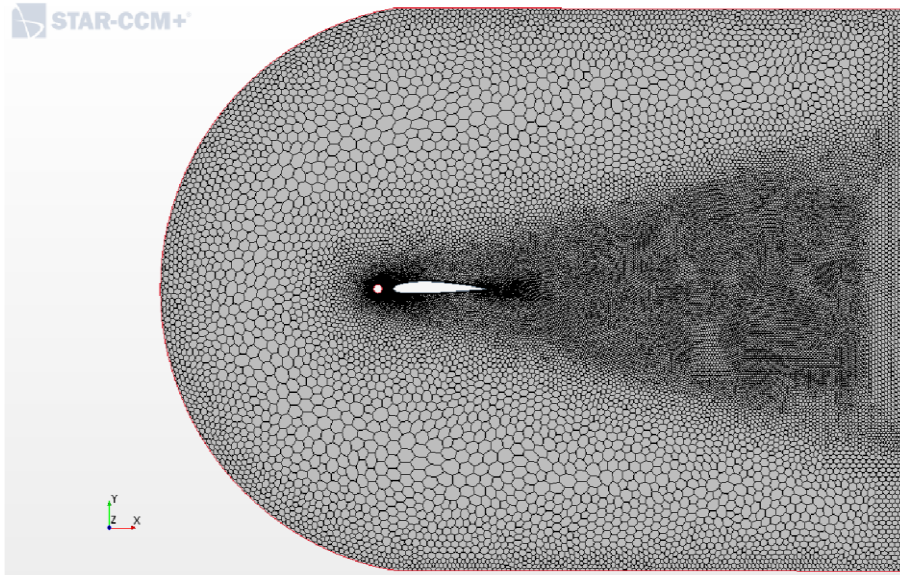


Fig. 2. Mesh used in simulation with emitter at zero degrees.

3 Results

3.1 Emitter in line with airfoil

Figures 3, 4 and 5 show the velocity, pressure and streamlines of the airflow, respectively, when 4kV is supplied to the wire, which is 12mm upstream of the airfoil.

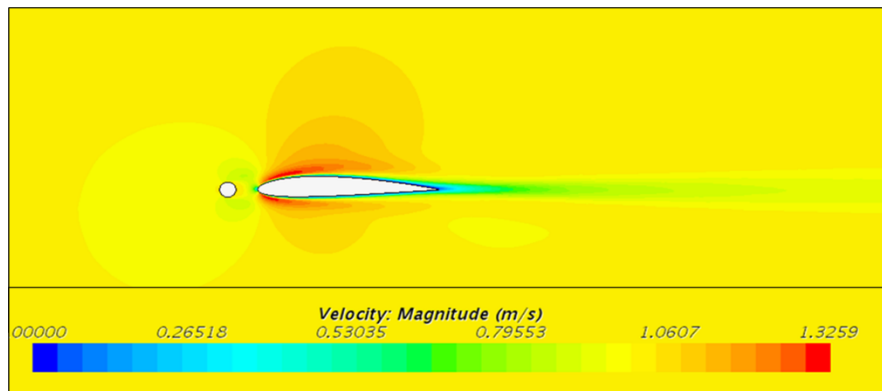


Fig. 3. Velocity profile when distance is set to 12mm and voltage to 4kV

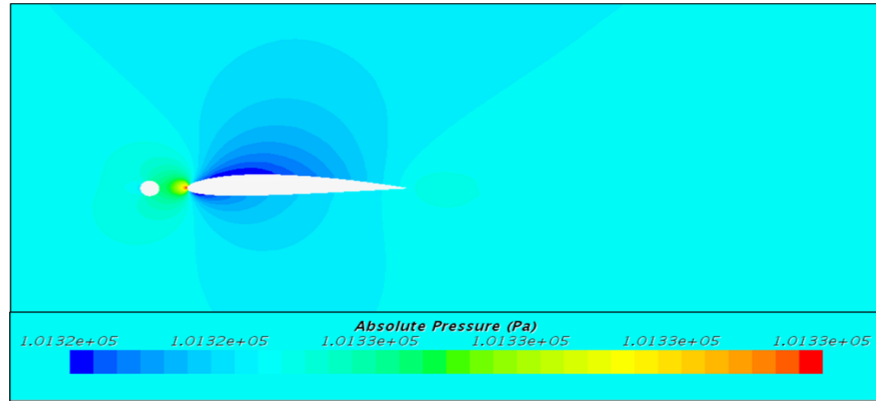


Fig. 4. Pressure profile when distance is set to 12mm and voltage to 4kV

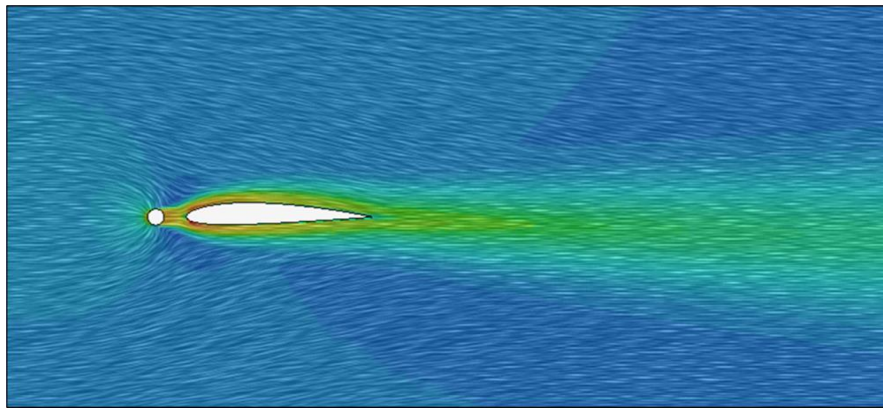


Fig. 5. Vector stream lines showing how the ionic wind flows from an ionization region to and over the airfoil.

The velocity and pressure profiles are not dis-similar to a standard distribution without the wire. However, the stagnation point is slightly higher in our model. Figure 5 shows the streamlines of the airflow emitted from the ionization region flow which is directed towards and diverted around the airfoil. Due to the close proximity of the emitter wire the airflow is concentrated at the tip of the airfoil rather than a consistent airflow being applied to the airfoil. This creates a stagnation pressure at a higher than normal location on the leading edge of the airfoil.

3.2 Emitter at various vertical displacements

The emitter was tested at different vertical displacements from the airfoil to evaluate the effect on values produced for the lift and drag of the airfoil. This variation in vertical height corresponds to a change in local flow direction in order to assess if there is an optimal position to place the emitter in terms of the aerodynamic performance. The horizontal position was kept constant, and the vertical position varied between -0.005m

and 0.005m in intervals of 0.0025m. Figure 6 reveals the results obtained in lift/drag due to ionization from the emitter at different positions on the y-axis.

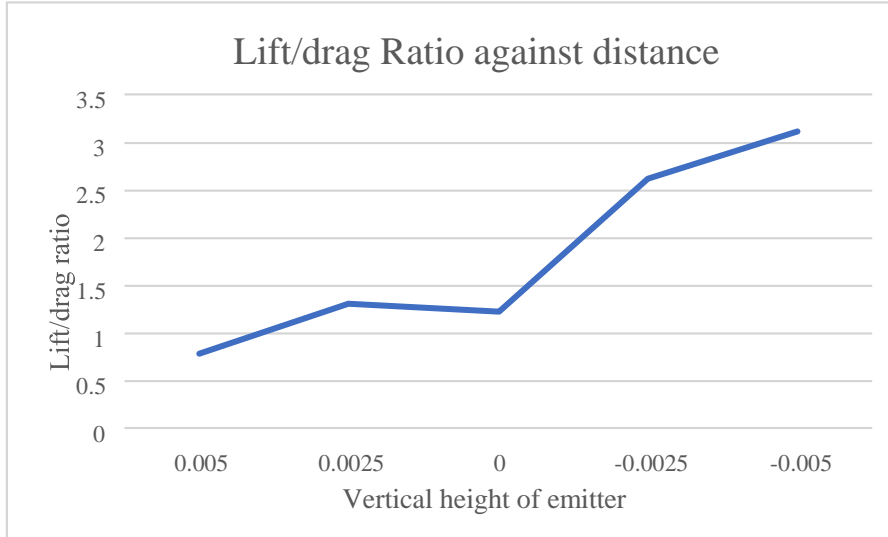


Fig. 6. Graph comparing the distance in the y-axis to the lift/drag ratio

Figure 6 appears to show a more favorable position for the emitter than the original horizontal location. The original horizontal position generated an extra lift of 0.00443 N and an extra drag of 0.00366 N when compared with the airfoil without the wire. However, at the lowest position studied of -0.005m, an extra lift of 0.0178 N and an extra drag of 0.00571 N was generated. This resulted in an extra lift/drag ratio of 3.11 compared to 1.21 generated when the emitter was horizontally in front of the airfoil. Therefore, the highest lift/drag ratio found is at a vertical distance -0.005m and is then followed by 0.0025m. The lowest lift/drag ratio is at a vertical distance 0.005m and is followed by the distance 0m. This means that when the emitter is placed below the airfoil, so at a vertical distance below 0m, the values for lift significantly increased whilst drag slightly increased hence a greater lift/drag ratio. As the position of the emitter was changed, the size and frequency of the vortices also changed. The lift values are greater at emitter distances lower in the y-axis due to greater induced angle of attack.

A trend can be seen in Figure 6, and it is predicted that for further values of distance in the y-axis below the airfoil will generate more lift until a critical distance has been met. Once this critical distance is reached, the lift will no longer increase as the emitter could be too far away from the airfoil for the positively charged ions to be attracted to the collector on the airfoil.

4 Conclusion

The ionic wind has been modelled around an airfoil. This was studied to see if the development of using ionic propulsion can be seen as an easier alternative of powering engines for in-atmosphere aircrafts, whilst considering its cost-effectiveness and the impact it has on the global environment. Through the use of CFD simulations, the airfoil and wire model has been tested and the results obtained from this model have been used to determine the extra lift and drag created from the ionic wind. The voltage used here is a magnitude lower than that used by MIT. This relatively low voltage was used to validate findings with previous experimental work but has led to a low induced velocity, which is insufficient to sustain flight at this scale. Increased voltages are needed at this model scale and much higher for the larger scale required for manned flight. In addition to greater values of voltage, further simulations with various electrode spacings and more vertical positions of the emitter could result in further improvements in performance. The results from changing the vertical position of the emitter showed that more lift could be generated by placing the emitter below the airfoil, whilst maintaining a spacing length of 12 ± 1 mm. Simulating the airflow at various angles of attack should also be evaluated as well as more work on the methodology to simulate the ionic wind. With further research, the methodology can be further developed and tailored to highlight how applicable an ionic engine could be in use for commercial airliners or military aircraft. Nevertheless, this project provides insight in developing ionic engine designs for in-atmosphere uses at small scales such as micro UAVs. However, significant work is required before this application can be used commercially to develop an in-atmosphere ionic engine.

References

1. Hall S.J., Jorns B.A., Gallimore A.D. and Goebel D.M.: Operation of a High-Power Nested Hall Thruster with Reduced Cathode Flow Fraction. *Journal of Propulsion and Power*, 36(6), 912–919 (2020).
2. Zhang, Y., Liu, L., Chen, Y., & Ouyang, J. Characteristics of ionic wind in needle-to-ring corona discharge. *Journal of Electrostatics*, 74, 15-20 (2015).
3. Xu, H., He, Y., Strobel, K.L., Gilmore, C.K., Kelley, S.P., Hennick, C.C., & Barrett, S.R.: Flight of an aeroplane with solid-state propulsion. *Nature*, 563(7732), 532-535 (2018).
4. Electron Air LLC Homepage, <https://electronairllc.org/>, last accessed 2023/5/18
5. Krauss, E. D. *US10119527B2 - self contained ion powered aircraft*. Google Patents. <https://patents.google.com/patent/US10119527B2/en>
6. Krauss, E. D. *US11161631B2 - ion propelled vehicle*. Google Patents. <https://patents.google.com/patent/US11161631B2/en>
7. Massachusetts Institute of Technology, <https://news.mit.edu/2018/first-ionic-wind-plane-no-moving-parts-1121>, last accessed 2023/5/18
8. He, Y., & Perreault, D.J.: Lightweight High-Voltage Power Converters for Electroaerodynamic Propulsion. *IEEE Journal of Emerging and Selected Topics in Industrial Electronics*, 2(4), 453-463 (2021).

9. Xu, H., He, Y., Strobel, K. L., Gilmore, C. K., Kelley, S. P., Hennick, C. C., Sebastian, T., Woolston, M. R., Perreault, D. J., & Barrett, S. R. H. (2018, November 21). *Flight of an aeroplane with solid-state propulsion*. Nature News. <https://www.nature.com/articles/s41586-018-0707-9>
10. Wilson, J., Perkins, H.D., & Thompson, W.K.: An investigation of ionic wind propulsion. No. NASA/TM-2009-215822, (2009).